Acta Cryst E CRYSTALLOGRAPHIC COMMUNICATIONS
ISSN 2056-9890

A triclinic polymorph of tricyclohexylphosphane sulfide: crystal structure and Hirshfeld surface analysis

Yi Jiun Tan,[a] Chien Ing Yeo,[a] Nathan R. Halcovitch,[b] Mukesh M. Jotani[c]‡ and Edward R. T. Tiekink[a]*

[a]Research Centre for Crystalline Materials, School of Science and Technology, Sunway University, 47500 Bandar Sunway, Selangor Darul Ehsan, Malaysia, [b]Department of Chemistry, Lancaster University, Lancaster LA1 4YB, United Kingdom, and [c]Department of Physics, Bhavan's Sheth R. A. College of Science, Ahmedabad, Gujarat 380001, India. *Correspondence e-mail: edwardt@sunway.edu.my

Received 4 March 2017
Accepted 4 March 2017

Edited by W. T. A. Harrison, University of Aberdeen, Scotland

‡ Additional correspondence author, e-mail: mmjotani@rediffmail.com.

Keywords: crystal structure; triorganophosphane sulfide; polymorph; Hirshfeld surface analysis.

CCDC reference: 1536014

Supporting information: this article has supporting information at journals.iucr.org/e

The title compound, $(C_6H_{11})_3PS$ (systematic name: tricyclohexyl-λ^5-phosphanethione), is a triclinic ($P\overline{1}$, Z' = 1) polymorph of the previously reported orthorhombic form (*Pnma*, Z' = 1/2) [Kerr *et al.* (1977). *Can. J. Chem.* **55**, 3081–3085; Reibenspies *et al.* (1996). *Z. Kristallogr.* **211**, 400]. While conformational differences exist between the non-symmetric molecule in the triclinic polymorph, *cf.* the mirror-symmetric molecule in the orthorhombic form, these differences are not chemically significant. The major feature of the molecular packing in the triclinic polymorph is the formation of linear chains along the *a* axis sustained by methine-C—H···S(thione) interactions. The chains pack with no directional interactions between them. The analysis of the Hirshfeld surface for both polymorphs indicates a high degree of similarity, being dominated by H···H (*ca* 90%) and S···H/H···S contacts.

1. Chemical context

Recent interest in the chemistry of phosphanegold(I) dithiocarbamate compounds stems from their potential as anti-cancer agents (de Vos *et al.* 2004; Ronconi *et al.* 2005; Gandin *et al.* 2010; Jamaludin *et al.* 2013; Keter *et al.* 2014; Altaf *et al.* 2015). In keeping with the increasing interest in gold compounds as potential anti-microbial agents to meet the challenges of microbes developing resistance to available chemotherapies (Glišić & Djuran, 2014) and in recognition of the potential of metal dithiocarbamates as anti-microbial agents (Hogarth, 2012), the anti-bacterial properties of phosphanegold(I) dithiocarbamates have also been explored in recent times (Sim *et al.*, 2014; Chen *et al.*, 2016). For example, the 'all-ethyl' compound, $Et_3PAu(S_2CNEt_2)$, exhibits broad-range activity against Gram-positive and Gram-negative bacteria and was shown to be bactericidal against methicillin-resistant *Staphylococcus aureus* (MRSA) (Chen *et al.*, 2016). As an extension of these studies, investigations into the anti-microbial potential of related bis(phosphane)copper(I) dithiocarbamates and their silver(I) analogues were undertaken, again revealing interesting results and dependency of activity upon phosphane- and dithiocarbamate-bound substituents (Jamaludin *et al.*, 2016). During further investigations in this field, the title compound, $Cy_3P{=}S$ (I), was isolated as a decomposition product from a long-term (months) recrystallization of an acetone solution containing $(Cy_3P)_2Ag(S_2CNEt_2)$. The crystal and molecular structures of

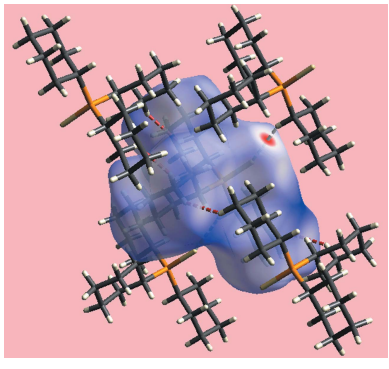

(I) are reported herein and the results compared with those of a previously determined orthorhombic polymorph, (II) (Kerr *et al.*, 1977; Reibenspies *et al.*, 1996). Further, a detailed comparison of the Hirshfeld surfaces for (I) and (II) is presented.

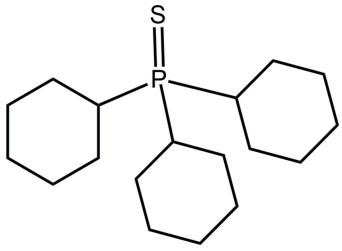

2. Structural commentary

The molecular structure of (I), Fig. 1, features a tetrahedrally coordinated P^V centre defined by a thione-S and three α-carbon atoms of the cyclohexyl substituents. The P1—C bond lengths span an experimentally distinct range of 1.8350 (14) to 1.8468 (15) Å, Table 1. The distortions from the ideal tetrahedral geometry are relatively minor with the widest angles generally involving the thione-S atom. The cyclohexyl rings, each with a chair conformation, adopt orientations so that the methine-H atom is directed towards the thione-S atom in the cases of the C1- and C13-rings, *i.e.* are *syn*, with that of the C7-ring being *anti*.

As mentioned above, the structure of (I) has been reported previously in an orthorhombic form in two separate determinations (Kerr *et al.*, 1977; Reibenspies *et al.*, 1996). Data from the more recent determination, measured at 163 K (Reibenspies *et al.*, 1996), are included in Table 1. The major difference in (II) is that the molecule lies on a crystallographic mirror plane; the 2 × *syn* plus 1 × *anti*-conformation of the methine-H atoms with respect to the thione-S atom persists. In (II), the P—C bond lengths are equal within experimental error. However, differences are apparent in the bond angles subtended at the P^V centre whereby the angles in (II) span a wider range, *i.e.* 8.5°, *cf.* 6.3 ° in (I). Also, the widest angle at the P1 atom in (II) is subtended by the symmetry-related cyclohexyl rings.

Table 1
Geometric parameters (Å, °) for the triclinic (I) and orthorhombic (II) polymorphs of $Cy_3P{=}S$.

Parameter	triclinic polymorph	orthorhombic polymorph[a]
P1═S1	1.9548 (5)	1.9612 (11)
P1—C1	1.8435 (14)	1.842 (3)
P1—C7	1.8350 (14)	1.836 (2)
P1—C13	1.8468 (15)	1.836 (2)
S1—P1—C1	109.99 (5)	112.16 (11)
S1—P1—C7	112.11 (5)	110.15 (7)
S1—P1—C13	111.60 (5)	110.15 (7)
C1—P1—C7	105.82 (6)	105.22 (9)
C1—P1—C13	105.70 (6)	105.22 (9)
C7—P1—C13	111.43 (6)	113.80 (10)

An overlay diagram for (I) and (II) is shown in Fig. 2, which highlights the coincidence of the cyclohexyl ring associated with the methine-H atom having the *anti*-disposition with respect to the thione-S atom. Clearly, there are conformational differences apparent between the cyclohexyl rings related across the pseudo- and crystallographic mirror planes in (I) and (II), respectively.

3. Supramolecular features

The only directional supramolecular interactions in the crystal of (I) identified in *PLATON* (Spek, 2009) are methine-C—

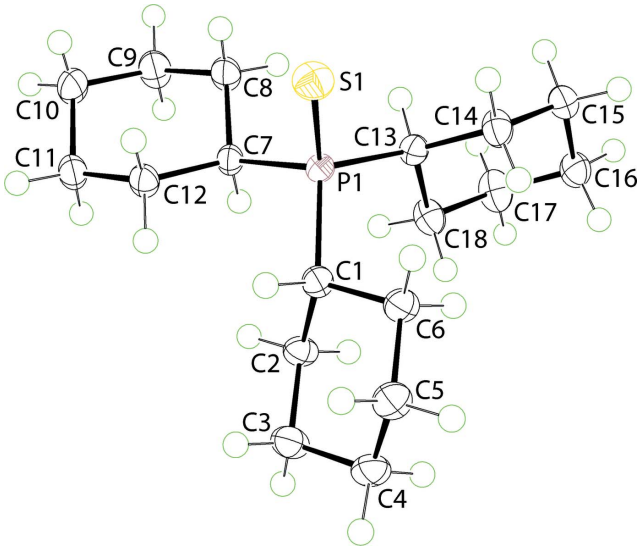

Figure 1
The molecular structure of polymorph (I), showing the atom-labelling scheme and displacement ellipsoids at the 70% probability level.

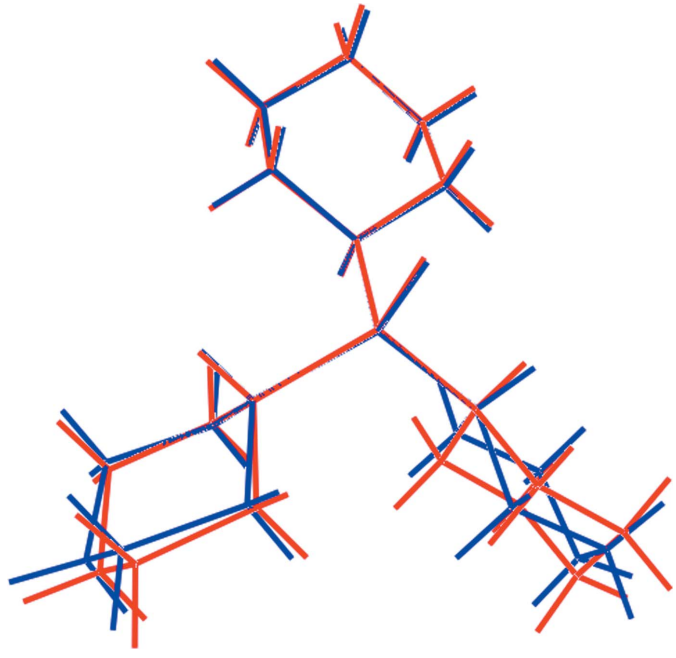

Figure 2
Overlay diagram of polymorphs (I), red image, and (II), blue image. The molecules are overlapped so the three α-C atoms of the cyclohexyl rings are coincident.

Table 2
Hydrogen-bond geometry (Å, °).

D—H···A	D—H	H···A	D···A	D—H···A
C7—H7···S1^{i}	1.00	2.65	3.5961 (14)	157

Symmetry code: (i) $x+1, y, z$.

H7···S(thione) contacts, *i.e.* involving the *anti*-disposed thione-S and methine-H atoms, Table 2. These lead to a linear chain aligned along the *a* axis as illustrated in Fig. 3*a*. The chains pack with no directional interactions between them, Fig. 3*b*.

In the original report of polymorph (II), it was stated '*There are no unusual inter-molecular contacts*' (Kerr *et al.*, 1977); no comment on the molecular packing was made in the redetermination (Reibenspies *et al.*, 1996). As seen from Fig. 4, supramolecular zigzag chains are evident in the molecular packing of (II), but these are sustained by weak methylene-C—H···S(thione) interactions [H···S^{i} = 3.027 (2) Å, C···S^{i} = 3.938 (2) Å with the angle at H = 159° for (i) $1+x, y, z$] formed on either side of the mirror plane, so the sulfur atom forms two such contacts, and propagate along the *a* axis.

A more detailed analysis of the molecular packing in (I) and (II) is given in *Hirshfeld surface analysis*.

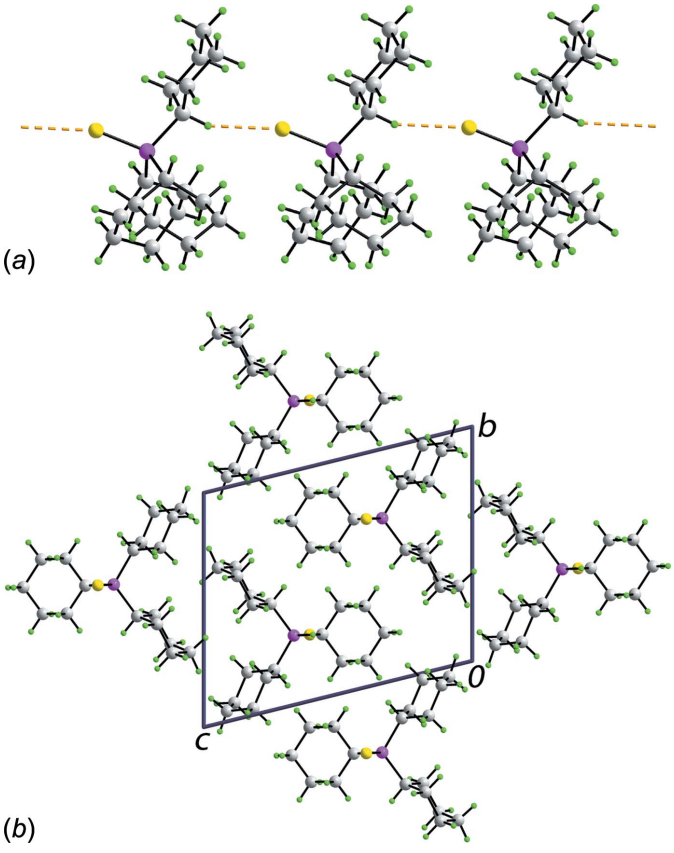

Figure 3
Molecular packing in polymorph (I), showing (*a*) a linear supramolecular chain mediated by methine-C—H···S(thione) interactions aligned along the *a* axis and (*b*) a view of the unit-cell contents in projection down the *a* axis. The C—H···S interactions are shown as orange dashed lines.

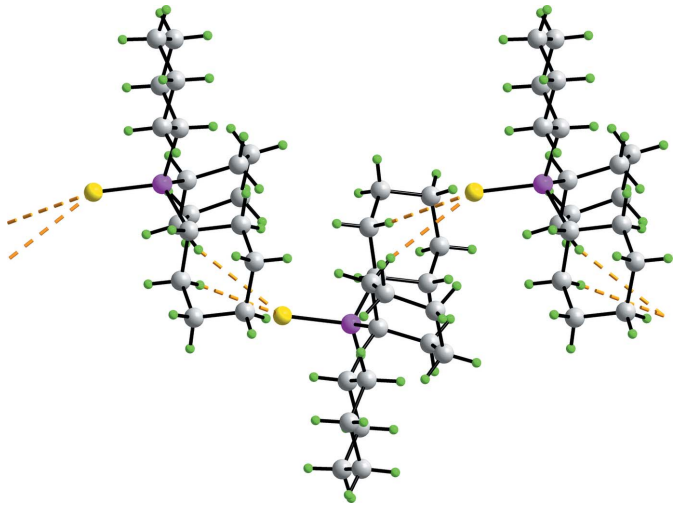

Figure 4
Molecular packing in polymorph (II), showing a zigzag supramolecular chain along the *a* axis mediated by methylene-C—H···S(thione) interactions, shown as orange dashed lines.

4. Hirshfeld surface analysis

In order to gain more insight into the molecular packing found in (I) and (II), the structures were subjected to a Hirshfeld surface analysis which was performed as described in a recent publication (Jotani *et al.*, 2016).

The different shapes of Hirshfeld surfaces mapped over electrostatic potential in Fig. 5 are indicative of the different molecular conformations adopted by the cyclohexane rings in

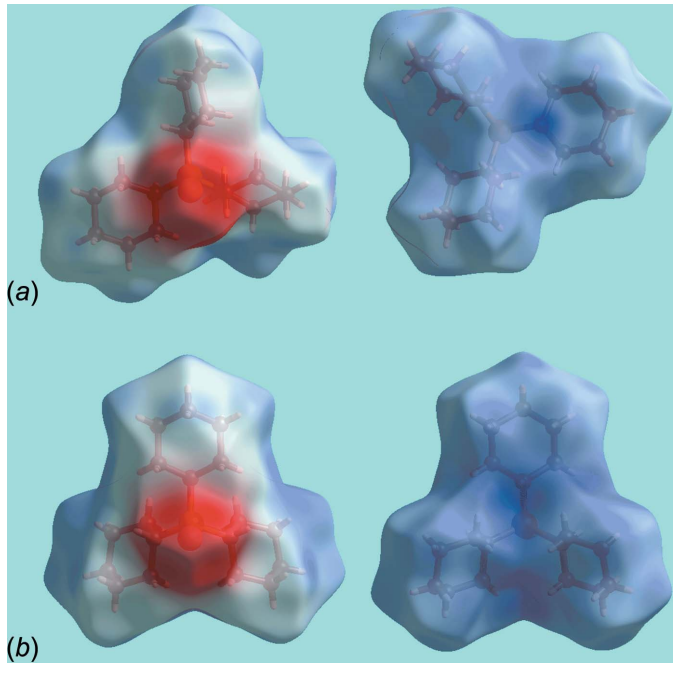

Figure 5
Views of the Hirshfeld surfaces for mapped over the electrostatic potential in the range ±0.075 au for (*a*) polymorph (I) and (*b*) polymorph (II).

Table 3
Percentage contributions of the different intermolecular contacts to the Hirshfeld surface in (I) and (II).

Contact	% contribution in (I)	% contribution in (II)
H···H	89.8	88.8
S···H/H···S	10.2	11.2

Table 4
Short interatomic contacts in (I).

Contact	distance	symmetry operation
H6*A*···H15*B*	2.32	$1-x, 1-y, 2-z$
H10*B*···H15*A*	2.37	$1-x, 1-y, 1-z$

(I) and (II). A pair of bright-red spots appearing on the Hirshfeld surface mapped over d_{norm} near methine-H7 and thione-S1 for (I), Fig. 6, on the extremities of the molecule represent the donor and acceptor of the C—H···S interaction, Table 2. They are viewed as the respective blue (positive) and red (negative) regions on the Hirshfeld surface mapped over electrostatic potential, Fig. 5. The absence of characteristic spots on the d_{norm}-mapped Hirshfeld surfaces in the orthorhombic polymorph (II) (not shown) indicates no similar interactions within the sum of the van der Waals radii; see below. The immediate environments about reference molecules of (I) and (II) within the d_{norm}-mapped Hirshfeld surfaces showing intermolecular C—H···S interactions are displayed in Fig. 7*a* and *b*, respectively. In the crystal of (II), the zigzag chain of weak intermolecular methylene-C—H···S(thione) contacts on either side of the crystallographic mirror plane is viewed as the pair of red dashed lines in Fig. 7*b* (see above).

The overall two-dimensional fingerprint plots for (I) and (II), and those delineated into H···H and S···H/H···S contacts (McKinnon *et al.*, 2007) are illustrated in Fig. 8. It is interesting to note that in both polymorphs only sulfur and hydrogen atoms lie on the periphery of the Hirshfeld surfaces and contribute to interatomic contacts such as they are; the percentage contributions are as quantified in Table 3. The different relative orientations of the cyclohexane rings in the two forms are also evident through the distinct distribution of points in their respective two-dimensional fingerprint plots,

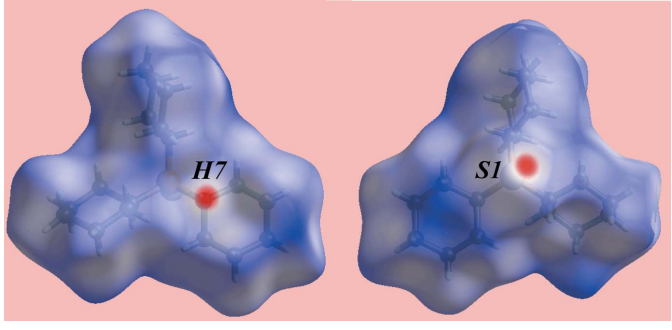

Figure 6
Views of the Hirshfeld surface for polymorph (I) mapped over d_{norm} over the range −0.160 to 1.823 au.

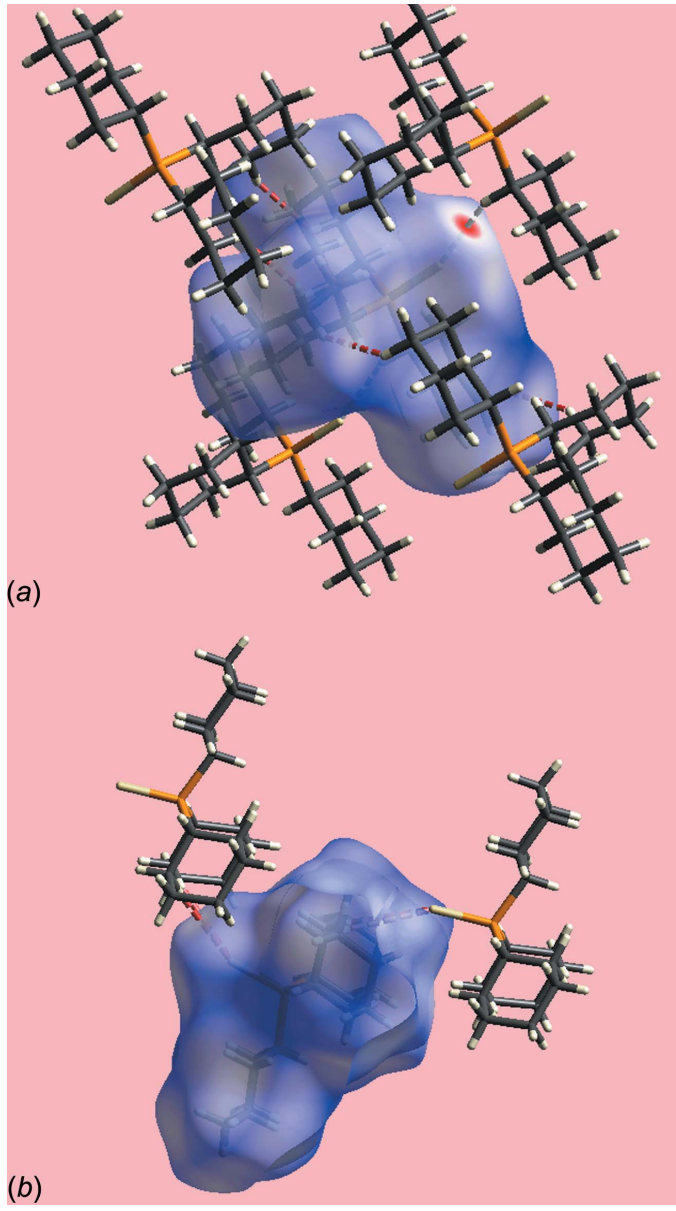

Figure 7
Views of the Hirshfeld surfaces mapped over d_{norm} about a reference molecule highlighting intermolecular C—H···S interactions and short interatomic H···H contacts as white and red dashed lines, respectively, for (*a*) polymorph (I) and (*b*) polymorph (II).

Fig. 8*a*. In particular for (II), Fig. 8*a*, the top region, corresponding to donor interactions is stunted with respect to the lower, acceptor region. For (I), a pair of small peaks at $d_e + d_i < 2.4$ Å in the fingerprint plot delineated into H···H contacts, Fig. 8*b*, show the contribution from short interatomic H···H contacts in the molecular packing, Table 4. This contrasts the situation for (II), where the pair of peaks occur at $d_e + d_i > 2.4$ Å, *i.e.* at separations greater than the sum of van der Waals radii. The relative strength of the intermolecular C—H···S interactions in (I) and (II) are characterized from the fingerprint plots delineated into S···H/H···S contacts, Fig. 8*c*, through the pair of spikes at $d_e + d_i \sim 2.7$ Å and $d_e + d_i \sim 3.1$ Å, respectively. The asym-

Table 5
Physiochemical properties for polymorphs (I) and (II).

Property	(I)	(II)
Volume, V (Å^3)	436.83	430.96
Surface area, A (Å^2)	351.03	345.83
A:V (Å^{-1})	0.804	0.802
Globularity, G	0.793	0.798
Asphericity, Ω	0.051	0.046
Density (g cm^{-3})	1.170	1.186
Packing index (%)	68.6	68.4

metric distribution of points in the fingerprint plot delineated into S···H/H···S contacts for (II) in Fig. 8*c* is the result of the orientation of the cyclohexane rings with respect to the crystallographic mirror plane. The upper region, corresponding to donor H···S contacts, contributes 4.7% to the surface *cf.* 6.5% in the lower region, corresponding to S···H acceptor contacts.

The similarity in the molecular packing of (I) and (II) is reflected in the similarity in the physiochemical data collated in Table 5 and calculated in *Crystal Explorer* (Wolff *et al.*, 2012) and *PLATON* (Spek, 2009). While it is noted the values are very close for (I) and (II) (Table 5), the volume of the molecule in (I) is slightly greater than that in (II), as is the surface area. However, the molecule in (II) is marginally more globular and reflecting the lack of directional interactions between molecules, allowing a closer approach, the density is greater than in (I). Nevertheless, the packing efficiency is marginally greater in (I), probably reflecting the lack of symmetry in the molecule *cf.* (I).

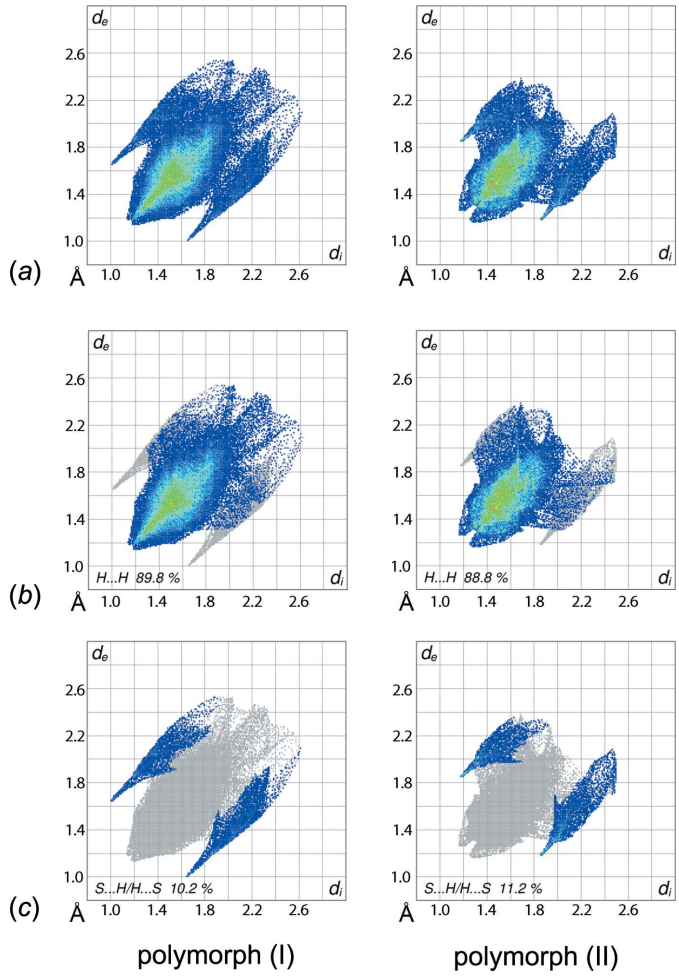

Figure 8
Fingerprint plots for polymorph (I) and polymorph (II), showing (*a*) overall and those delineated into (*b*) H···H and (*c*) S···H/H···S contacts.

5. Database survey

There are a number of triorganophosphane sulfide structures in the crystallographic literature (Groom *et al.*, 2016) with those conforming to the general formula R_3P═S being summarized here. Thus, structures have been described with fractional atomic coordinates, for example with R = Me (Tasker *et al.*, 2005), *i*Pr (Staples & Segal, 2001), *t*Bu (Steinberger *et al.*, 2001), Ph (Foces-Foces & Llamas-Saiz, 1998; monoclinic polymorph), Ph (Ziemer *et al.*, 2000; triclinic

Table 6
Geometric parameters (Å, °) for selected R_3P═S molecules.

R	P═S	S—P—C	C—P—C	Reference
Me[a]	1.9664 (7)	112.88 (6)–113.22 (8)	105.33 (8)–106.53 (8)	Tasker *et al.*, 2005
*i*Pr[a]	1.926 (3)	110.08 (19)–112.3 (2)	103.88 (19)–116.3 (4)	Staples *et al.*, 2001
*t*Bu[b]	1.9627 (15)	109.29 (14)	109.65 (19)	Steinberger *et al.*, 2001
Ph[c,d]	1.9554 (7)	112.16 (6)–113.47 (6)	103.70 (8)–107.76 (8)	Foces-Foces & Llamas-Saiz, 1998
	1.9547 (7)	112.28 (7)–113.67 (6)	103.12 (8)–107.53 (9)	
Ph[d,e]	1.9544 (9)	112.47 (7)–113.99 (7)	103.43 (8)–106.83 (8)	Ziemer *et al.*, 2000
	1.9529 (8)	111.97 (7)–113.19 (7)	103.61 (8)–107.38 (8)	
2-tolyl[d]	1.953 (6)	110.7 (3)–114.2 (3)	101.4 (3)–110.6 (4)	Cameron & Dahlèn, 1975
	1.942 (5)	111.6 (2)–114.3 (2)	104.9 (3)–107.9 (3)	
3-tolyl	1.937 (4)	112.1 (8)–112.6 (4)	105.5 (7)–108.2 (10)	Cameron *et al.*, 1978
4-FPh	1.9540 (9)	113.27 (8)–113.59 (8)	104.97 (10)–105.92 (10)	Barnes *et al.*, 2007
2,4,6-Me_3Ph	1.9748 (13)	107.32 (11)–109.49 (12)	108.90 (16)–112.45 (15)	Garland *et al.*, 2013
2,4,6-$(OMe)_3$Ph	1.9619 (12)	109.22 (11)–116.15 (11)	100.77 (14)–110.58 (14)	Finnen *et al.*, 1994
2-$(Me_2NCH_2)_3$Ph	1.9622 (17)	110.66 (8)–116.15 (10)	103.51 (13)–106.33 (11)	Rotar *et al.*, 2010
Cy[a,f]	1.9612 (11)	110.15 (7)–112.16 (11)	105.22 (9)–113.80 (10)	Reibenspies *et al.*, 1996
Cy[e]	1.9548 (5)	109.99 (5)–112.11 (5)	105.70 (6)–111.43 (6)	this work

Notes: (*a*) The molecule has crystallographic mirror symmetry with the S1, P1 and C1 atoms lying on the plane; (*b*) the molecule has crystallographic threefold symmetry with the S1 and P1 atoms lying on the axis; (*c*) monoclinic polymorph; (*d*) two independent molecules in the asymmetric unit; (*e*) triclinic polymorph; (*f*) orthorhombic polymorph.

polymorph), 2-tolyl (Cameron & Dahlèn, 1975), 3-tolyl (Cameron *et al.*, 1978), 4-FPh (Barnes *et al.*, 2007), 2-$(Me_2NCH_2)_3$Ph (Rotar *et al.*, 2010), 2,4,6-Me_3Ph (Garland *et al.*, 2013) and 2,4,6-$(OMe)_3$Ph (Finnen *et al.*, 1994). Selected geometric data for these structures along with those for (I) and (II) are collected in Table 6. The *R* = Me and *i*Pr molecules have crystallographic mirror symmetry as for (II) whereas the *R* = *t*Bu compound has crystallographically imposed threefold symmetry. Two polymorphs have been found for *R* = Ph, and each of these features two independent molecules in the asymmetric unit.

The longest P═S bond length, *i.e.* 1.9748 (13) Å, is found in sterically encumbered (2,4,6-Me3Ph)$_3$P═S (Garland *et al.*, 2013). That steric effects are not the only factors influencing the magnitude of the P═S bond length is realized in the structure of Me_3P═S, with small, electron-donating groups, which has the second longest P═S bond length across the series. The comments on the lack of definitive trends in the S—P—C and C—P—C bond angles made above for (I) and (II) hold true across the series although, generally, the former are wider than the latter. Interestingly, in the threefold symmetric *t*Bu_3P═S structure, all angles are about 109°.

6. Synthesis and crystallization

The title compound (I) is an unexpected product from the *in situ* reaction of $(Cy_3P)_2$AgCl with Na[S_2CNEt_2] in a 2:1 ratio. The preparation was as follows: Cy_3P (Sigma–Aldrich; 0.6 mmol, 0.196 g) dissolved in acetone (20 ml) was added to an acetone solution (20 ml) of AgCl (Sigma–Aldrich; 0.3 mmol, 0.05 g) at room temperature. Then, Na[S_2CNEt_2] (BDH, 0.3 mmol, 0.08 g) in acetone (20 ml) was added to the reaction mixture followed by stirring for 4 h. The resulting mixture was filtered, covered to exclude light and left for evaporation at room temperature. Colourless crystals were obtained after four months. Yield: 0.132 g (55%), m.p.: 437–440 K. IR (cm^{-1}): ν(P═S) 624 (*s*).

7. Refinement

Crystal data, data collection and structure refinement details are summarized in Table 7. Carbon-bound H atoms were placed in calculated positions (C—H = 0.99–1.00 Å) and were included in the refinement in the riding-model approximation, with U_{iso}(H) set to 1.2U_{eq}(C).

Acknowledgements

The authors are grateful to Sunway University (INT-RRO-2017–096) for supporting this research.

Table 7
Experimental details.

Crystal data	
Chemical formula	$C_{18}H_{33}PS$
M_r	312.47
Crystal system, space group	Triclinic, $P\overline{1}$
Temperature (K)	100
a, *b*, *c* (Å)	6.6400 (5), 10.8089 (9), 12.8818 (10)
α, β, γ (°)	103.430 (7), 98.467 (7), 91.912 (7)
V (Å^3)	887.26 (12)
Z	2
Radiation type	Mo *K*α
μ (mm^{-1})	0.26
Crystal size (mm)	0.40 × 0.20 × 0.17
Data collection	
Diffractometer	Agilent SuperNova, Dual, Mo at zero, AtlasS2
Absorption correction	Multi-scan (*CrysAlis PRO*; Rigaku Oxford Diffraction, 2015)
T_{min}, T_{max}	0.926, 1.000
No. of measured, independent and observed [$I > 2\sigma(I)$] reflections	8658, 4208, 3739
R_{int}	0.022
(sin $\theta/\lambda)_{max}$ (Å^{-1})	0.696
Refinement	
$R[F^2 > 2\sigma(F^2)]$, $wR(F^2)$, *S*	0.037, 0.097, 1.01
No. of reflections	4208
No. of parameters	181
H-atom treatment	H-atom parameters constrained
$\Delta\rho_{max}$, $\Delta\rho_{min}$ (e Å^{-3})	0.47, −0.35

Computer programs: *CrysAlis PRO* (Rigaku Oxford Diffraction, 2015), *SHELXS97* (Sheldrick, 2008), *SHELXL2014* (Sheldrick, 2015), *ORTEP-3 for Windows* (Farrugia, 2012), *QMol* (Gans & Shalloway, 2001), *DIAMOND* (Brandenburg, 2006) and *publCIF* (Westrip, 2010).

References

Altaf, M., Monim-ul-Mehboob, M., Seliman, A. A. A., Sohail, M., Wazeer, M. I. M., Isab, A. A., Li, L., Dhuna, V., Bhatia, G. & Dhuna, K. (2015). *Eur. J. Med. Chem.* **95**, 464–472.

Barnes, N. A., Godfrey, S. M., Halton, R. T. A., Khan, R. Z., Jackson, S. L. & Pritchard, R. G. (2007). *Polyhedron*, **26**, 4294–4302.

Brandenburg, K. (2006). *DIAMOND*. Crystal Impact GbR, Bonn, Germany.

Cameron, T. S. & Dahlèn, B. (1975). *J. Chem. Soc. Perkin Trans. 2*, pp. 1737–1751.

Cameron, T. S., Howlett, K. D. & Miller, K. (1978). *Acta Cryst.* B**34**, 1639–1644.

Chen, B.-J., Jamaludin, N. S., Khoo, C.-H., See, T.-H., Sim, J.-H., Cheah, Y.-K., Halim, S. N. A., Seng, H.-L. & Tiekink, E. R. T. (2016). *J. Inorg. Biochem.* **163**, 68–80.

Farrugia, L. J. (2012). *J. Appl. Cryst.* **45**, 849–854.

Finnen, D. C. & Pinkerton, A. A. (1994). *Phosphorus Sulfur Silicon Relat. Elem.* **90**, 11–19.

Foces-Foces, C. & Llamas-Saiz, A. L. (1998). *Acta Cryst*. (1998). C**54**, IUC9800013.

Gandin, V., Fernandes, A. P., Rigobello, M. P., Dani, B., Sorrentino, F., Tisato, F., Björnstedt, M., Bindoli, A., Sturaro, A., Rella, R. & Marzano, C. (2010). *Biochem. Pharmacol.* **79**, 90–101.

Gans, J. & Shalloway, D. (2001). *J. Mol. Graphics Modell.* **19**, 557–559.

Garland, J., Slawin, A. M. Z. & Woollins, J. D. (2013). Private communication (refcode ZIVRAZ). CCDC, Cambridge, England.

Glišić, B. Đ. & Djuran, M. I. (2014). *Dalton Trans.* **43**, 5950–5969.

Groom, C. R., Bruno, I. J., Lightfoot, M. P. & Ward, S. C. (2016). *Acta Cryst.* B**72**, 171–179.

Hogarth, G. (2012). *Mini Rev. Med. Chem.* **12**, 1202–1215.

Jamaludin, N. S., Goh, Z.-J., Cheah, Y. K., Ang, K.-P., Sim, J. H., Khoo, C. H., Fairuz, Z. A., Halim, S. N. A., Ng, S. W., Seng, H.-L. & Tiekink, E. R. T. (2013). *Eur. J. Med. Chem.* **67**, 127–141.

Jamaludin, N. S., Halim, S. N. A., Khoo, C.-H., Chen, B.-J., See, T.-H., Sim, J.-H., Cheah, Y.-K., Seng, H.-L. & Tiekink, E. R. T. (2016). *Z. Kristallogr.* **231**, 341–349.

Jotani, M. M., Poplaukhin, P., Arman, H. D. & Tiekink, E. R. T. (2016). *Acta Cryst.* E**72**, 1085–1092.
Kerr, K. A., Boorman, P. M., Misener, B. S. & van Roode, J. H. G. (1977). *Can. J. Chem.* **55**, 3081–3085.
Keter, F. K., Guzei, I. A., Nell, M., van Zyl, W. E. & Darkwa, J. (2014). *Inorg. Chem.* **53**, 2058–2067.
McKinnon, J. J., Jayatilaka, D. & Spackman, M. A. (2007). *Chem. Commun.* pp. 3814–3816.
Reibenspies, J. H., Draper, J. D., Struck, G. & Darensbourg, D. J. (1996). *Z. Kristallogr.* **211**, 400.
Rigaku Oxford Diffraction (2015). *CrysAlis PRO*. Agilent Technologies Inc., Santa Clara, CA, USA.
Ronconi, L., Giovagnini, L., Marzano, C., Bettìo, F., Graziani, R., Pilloni, G. & Fregona, D. (2005). *Inorg. Chem.* **44**, 1867–1881.
Rotar, A., Covaci, A., Pop, A. & Silvestru, A. (2010). *Rev. Roum. Chim.* **55**, 823–829.
Sheldrick, G. M. (2008). *Acta Cryst.* A**64**, 112–122.
Sheldrick, G. M. (2015). *Acta Cryst.* C**71**, 3–8.
Sim, J.-H., Jamaludin, N. S., Khoo, C.-H., Cheah, Y.-K., Halim, S. N. A., Seng, H.-L. & Tiekink, E. R. T. (2014). *Gold Bull.* **47**, 225–236.
Spek, A. L. (2009). *Acta Cryst.* D**65**, 148–155.
Staples, R. J. & Segal, B. M. (2001). *Acta Cryst.* E**57**, o432–o433.
Steinberger, H.-U., Ziemer, B. & Meisel, M. (2001). *Acta Cryst.* C**57**, 835–837.
Tasker, P., Coventry, D., Parsons, S. & Messenger, D. (2005). Private communication (refcode METPHS01). CCDC, Cambridge, England.
Vos, D. de, Ho, S. Y. & Tiekink, E. R. T. (2004). *Bioinorg. Chem. Appl.* **2**, 141–154.
Westrip, S. P. (2010). *J. Appl. Cryst.* **43**, 920–925.
Wolff, S. K., Grimwood, D. J., McKinnon, J. J., Turner, M. J., Jayatilaka, D. & Spackman, M. A. (2012). *Crystal Explorer*. The University of Western Australia.
Ziemer, B., Rabis, A. & Steinberger, H.-U. (2000). *Acta Cryst.* C**56**, e58–e59.

supporting information

Acta Cryst. (2017). E**73**, 493-499 [https://doi.org/10.1107/S205698901700353X]

A triclinic polymorph of tricyclohexylphosphane sulfide: crystal structure and Hirshfeld surface analysis

Yi Jiun Tan, Chien Ing Yeo, Nathan R. Halcovitch, Mukesh M. Jotani and Edward R. T. Tiekink

Computing details

Data collection: *CrysAlis PRO* (Rigaku Oxford Diffraction, 2015); cell refinement: *CrysAlis PRO* (Rigaku Oxford Diffraction, 2015); data reduction: *CrysAlis PRO* (Rigaku Oxford Diffraction, 2015); program(s) used to solve structure: *SHELXS97* (Sheldrick, 2008); program(s) used to refine structure: *SHELXL2014* (Sheldrick, 2015); molecular graphics: *ORTEP-3 for Windows* (Farrugia, 2012), *QMol* (Gans & Shalloway, 2001) and *DIAMOND* (Brandenburg, 2006); software used to prepare material for publication: *publCIF* (Westrip, 2010).

Tricyclohexyl-λ^5-phosphanethione

Crystal data

$C_{18}H_{33}PS$
$M_r = 312.47$
Triclinic, $P\overline{1}$
$a = 6.6400$ (5) Å
$b = 10.8089$ (9) Å
$c = 12.8818$ (10) Å
$\alpha = 103.430$ (7)°
$\beta = 98.467$ (7)°
$\gamma = 91.912$ (7)°
$V = 887.26$ (12) Å^3
$Z = 2$
$F(000) = 344$
$D_x = 1.170$ Mg m^{-3}
Mo $K\alpha$ radiation, $\lambda = 0.71073$ Å
Cell parameters from 4800 reflections
$\theta = 3.7$–$29.5°$
$\mu = 0.26$ mm^{-1}
$T = 100$ K
Prism, colourless
0.40 × 0.20 × 0.17 mm

Data collection

Agilent SuperNova, Dual, Mo at zero, AtlasS2 diffractometer
Radiation source: micro-focus sealed X-ray tube, SuperNova (Mo) X-ray Source
Mirror monochromator
ω scans
Absorption correction: multi-scan (CrysAlis PRO; Rigaku Oxford Diffraction, 2015)
$T_{min} = 0.926$, $T_{max} = 1.000$
8658 measured reflections
4208 independent reflections
3739 reflections with $I > 2\sigma(I)$
$R_{int} = 0.022$
$\theta_{max} = 29.7°$, $\theta_{min} = 2.8°$
$h = -8 \rightarrow 9$
$k = -13 \rightarrow 12$
$l = -16 \rightarrow 17$

Refinement

Refinement on F^2
Least-squares matrix: full
$R[F^2 > 2\sigma(F^2)] = 0.037$
$wR(F^2) = 0.097$
$S = 1.01$
4208 reflections
181 parameters
0 restraints
Hydrogen site location: inferred from neighbouring sites
H-atom parameters constrained

$w = 1/[\sigma^2(F_o^2) + (0.0433P)^2 + 0.4808P]$
where $P = (F_o^2 + 2F_c^2)/3$
$(\Delta/\sigma)_{max} = 0.001$

$\Delta\rho_{max} = 0.47$ e Å^{-3}
$\Delta\rho_{min} = -0.35$ e Å^{-3}

Special details

Geometry. All esds (except the esd in the dihedral angle between two l.s. planes) are estimated using the full covariance matrix. The cell esds are taken into account individually in the estimation of esds in distances, angles and torsion angles; correlations between esds in cell parameters are only used when they are defined by crystal symmetry. An approximate (isotropic) treatment of cell esds is used for estimating esds involving l.s. planes.

Fractional atomic coordinates and isotropic or equivalent isotropic displacement parameters (Å²)

	x	*y*	*z*	U_{iso}*/U_{eq}
S1	0.28983 (5)	0.28303 (4)	0.60522 (3)	0.02266 (11)
P1	0.58024 (5)	0.29616 (3)	0.66467 (3)	0.01328 (10)
C1	0.6361 (2)	0.17062 (13)	0.73806 (11)	0.0155 (3)
H1	0.5711	0.0898	0.6877	0.019*
C2	0.8619 (2)	0.14502 (14)	0.76697 (12)	0.0176 (3)
H2A	0.9269	0.1300	0.7012	0.021*
H2B	0.9347	0.2205	0.8197	0.021*
C3	0.8780 (2)	0.02835 (15)	0.81546 (12)	0.0215 (3)
H3A	0.8173	−0.0484	0.7599	0.026*
H3B	1.0238	0.0157	0.8371	0.026*
C4	0.7689 (2)	0.04367 (15)	0.91382 (12)	0.0215 (3)
H4A	0.8396	0.1143	0.9727	0.026*
H4B	0.7751	−0.0355	0.9400	0.026*
C5	0.5457 (2)	0.07171 (15)	0.88609 (12)	0.0210 (3)
H5A	0.4708	−0.0033	0.8337	0.025*
H5B	0.4820	0.0873	0.9524	0.025*
C6	0.5286 (2)	0.18808 (14)	0.83768 (12)	0.0183 (3)
H6A	0.5910	0.2649	0.8927	0.022*
H6B	0.3828	0.2012	0.8168	0.022*
C7	0.7413 (2)	0.27103 (13)	0.55847 (11)	0.0151 (3)
H7	0.8872	0.2799	0.5940	0.018*
C8	0.7119 (2)	0.37069 (14)	0.49033 (12)	0.0209 (3)
H8A	0.5663	0.3672	0.4581	0.025*
H8B	0.7496	0.4570	0.5376	0.025*
C9	0.8424 (3)	0.34686 (15)	0.40031 (12)	0.0252 (3)
H9A	0.8170	0.4105	0.3565	0.030*
H9B	0.9886	0.3571	0.4325	0.030*
C10	0.7926 (3)	0.21275 (15)	0.32763 (12)	0.0254 (3)
H10A	0.8810	0.1984	0.2710	0.030*
H10B	0.6488	0.2042	0.2915	0.030*
C11	0.8260 (2)	0.11291 (14)	0.39418 (12)	0.0203 (3)
H11A	0.7889	0.0267	0.3465	0.024*
H11B	0.9721	0.1172	0.4257	0.024*
C12	0.6967 (2)	0.13517 (14)	0.48499 (11)	0.0178 (3)
H12A	0.7261	0.0720	0.5290	0.021*
H12B	0.5503	0.1224	0.4532	0.021*

C13	0.6633 (2)	0.45629 (13)	0.75178 (11)	0.0155 (3)
H13	0.6674	0.5136	0.7012	0.019*
C14	0.5091 (2)	0.51104 (15)	0.82558 (12)	0.0202 (3)
H14A	0.3716	0.5046	0.7820	0.024*
H14B	0.5027	0.4609	0.8804	0.024*
C15	0.5722 (2)	0.65042 (15)	0.88193 (12)	0.0219 (3)
H15A	0.5689	0.7014	0.8271	0.026*
H15B	0.4736	0.6838	0.9304	0.026*
C16	0.7857 (2)	0.66490 (14)	0.94750 (12)	0.0205 (3)
H16A	0.7863	0.6202	1.0064	0.025*
H16B	0.8246	0.7563	0.9807	0.025*
C17	0.9411 (2)	0.60985 (15)	0.87601 (13)	0.0242 (3)
H17A	1.0768	0.6154	0.9212	0.029*
H17B	0.9516	0.6609	0.8222	0.029*
C18	0.8796 (2)	0.47037 (14)	0.81713 (12)	0.0200 (3)
H18A	0.8846	0.4175	0.8706	0.024*
H18B	0.9779	0.4392	0.7678	0.024*

Atomic displacement parameters (Å²)

	U^{11}	U^{22}	U^{33}	U^{12}	U^{13}	U^{23}
S1	0.01585 (19)	0.0258 (2)	0.0254 (2)	0.00077 (14)	0.00114 (14)	0.00571 (15)
P1	0.01333 (18)	0.01384 (18)	0.01275 (17)	0.00045 (12)	0.00201 (12)	0.00351 (13)
C1	0.0171 (7)	0.0152 (7)	0.0156 (6)	0.0008 (5)	0.0049 (5)	0.0050 (5)
C2	0.0175 (7)	0.0190 (7)	0.0197 (7)	0.0038 (5)	0.0062 (5)	0.0090 (6)
C3	0.0237 (8)	0.0200 (8)	0.0248 (8)	0.0066 (6)	0.0081 (6)	0.0101 (6)
C4	0.0263 (8)	0.0204 (8)	0.0222 (7)	0.0040 (6)	0.0074 (6)	0.0116 (6)
C5	0.0240 (8)	0.0209 (8)	0.0217 (7)	0.0008 (6)	0.0083 (6)	0.0095 (6)
C6	0.0197 (7)	0.0197 (7)	0.0189 (7)	0.0034 (5)	0.0074 (5)	0.0084 (6)
C7	0.0200 (7)	0.0129 (7)	0.0130 (6)	0.0013 (5)	0.0047 (5)	0.0026 (5)
C8	0.0334 (8)	0.0140 (7)	0.0174 (7)	0.0034 (6)	0.0080 (6)	0.0054 (5)
C9	0.0427 (10)	0.0172 (8)	0.0207 (7)	0.0040 (6)	0.0140 (7)	0.0089 (6)
C10	0.0429 (10)	0.0208 (8)	0.0152 (7)	0.0069 (7)	0.0094 (6)	0.0061 (6)
C11	0.0293 (8)	0.0151 (7)	0.0169 (7)	0.0029 (6)	0.0066 (6)	0.0026 (5)
C12	0.0249 (7)	0.0129 (7)	0.0165 (7)	0.0009 (5)	0.0058 (5)	0.0039 (5)
C13	0.0162 (7)	0.0158 (7)	0.0146 (6)	0.0008 (5)	0.0029 (5)	0.0034 (5)
C14	0.0166 (7)	0.0219 (8)	0.0194 (7)	0.0024 (5)	0.0032 (5)	−0.0006 (6)
C15	0.0252 (8)	0.0205 (8)	0.0185 (7)	0.0075 (6)	0.0025 (6)	0.0012 (6)
C16	0.0250 (8)	0.0150 (7)	0.0194 (7)	−0.0003 (5)	0.0024 (6)	0.0004 (5)
C17	0.0205 (8)	0.0203 (8)	0.0282 (8)	−0.0052 (6)	0.0047 (6)	−0.0011 (6)
C18	0.0164 (7)	0.0177 (7)	0.0233 (7)	−0.0001 (5)	0.0028 (6)	0.0003 (6)

Geometric parameters (Å, º)

S1—P1	1.9548 (5)	C9—H9A	0.9900
P1—C1	1.8435 (14)	C9—H9B	0.9900
P1—C7	1.8350 (14)	C10—C11	1.529 (2)
P1—C13	1.8468 (15)	C10—H10A	0.9900

C1—C6	1.5356 (18)	C10—H10B	0.9900
C1—C2	1.5408 (19)	C11—C12	1.5302 (19)
C1—H1	1.0000	C11—H11A	0.9900
C2—C3	1.532 (2)	C11—H11B	0.9900
C2—H2A	0.9900	C12—H12A	0.9900
C2—H2B	0.9900	C12—H12B	0.9900
C3—C4	1.530 (2)	C13—C18	1.5376 (19)
C3—H3A	0.9900	C13—C14	1.5391 (19)
C3—H3B	0.9900	C13—H13	1.0000
C4—C5	1.530 (2)	C14—C15	1.527 (2)
C4—H4A	0.9900	C14—H14A	0.9900
C4—H4B	0.9900	C14—H14B	0.9900
C5—C6	1.529 (2)	C15—C16	1.523 (2)
C5—H5A	0.9900	C15—H15A	0.9900
C5—H5B	0.9900	C15—H15B	0.9900
C6—H6A	0.9900	C16—C17	1.527 (2)
C6—H6B	0.9900	C16—H16A	0.9900
C7—C8	1.540 (2)	C16—H16B	0.9900
C7—C12	1.5437 (19)	C17—C18	1.533 (2)
C7—H7	1.0000	C17—H17A	0.9900
C8—C9	1.528 (2)	C17—H17B	0.9900
C8—H8A	0.9900	C18—H18A	0.9900
C8—H8B	0.9900	C18—H18B	0.9900
C9—C10	1.528 (2)		

C7—P1—C1	105.82 (6)	C10—C9—H9B	109.5
C7—P1—C13	105.70 (6)	C8—C9—H9B	109.5
C1—P1—C13	111.43 (6)	H9A—C9—H9B	108.1
C7—P1—S1	112.11 (5)	C9—C10—C11	110.38 (12)
C1—P1—S1	109.99 (5)	C9—C10—H10A	109.6
C13—P1—S1	111.60 (5)	C11—C10—H10A	109.6
C6—C1—C2	110.75 (11)	C9—C10—H10B	109.6
C6—C1—P1	111.78 (10)	C11—C10—H10B	109.6
C2—C1—P1	117.32 (10)	H10A—C10—H10B	108.1
C6—C1—H1	105.3	C12—C11—C10	110.93 (12)
C2—C1—H1	105.3	C12—C11—H11A	109.5
P1—C1—H1	105.3	C10—C11—H11A	109.5
C3—C2—C1	110.13 (12)	C12—C11—H11B	109.5
C3—C2—H2A	109.6	C10—C11—H11B	109.5
C1—C2—H2A	109.6	H11A—C11—H11B	108.0
C3—C2—H2B	109.6	C11—C12—C7	111.43 (12)
C1—C2—H2B	109.6	C11—C12—H12A	109.3
H2A—C2—H2B	108.1	C7—C12—H12A	109.3
C4—C3—C2	111.72 (12)	C11—C12—H12B	109.3
C4—C3—H3A	109.3	C7—C12—H12B	109.3
C2—C3—H3A	109.3	H12A—C12—H12B	108.0
C4—C3—H3B	109.3	C18—C13—C14	110.45 (11)
C2—C3—H3B	109.3	C18—C13—P1	115.68 (10)

H3A—C3—H3B	107.9	C14—C13—P1	113.42 (10)
C3—C4—C5	111.30 (12)	C18—C13—H13	105.4
C3—C4—H4A	109.4	C14—C13—H13	105.4
C5—C4—H4A	109.4	P1—C13—H13	105.4
C3—C4—H4B	109.4	C15—C14—C13	110.25 (12)
C5—C4—H4B	109.4	C15—C14—H14A	109.6
H4A—C4—H4B	108.0	C13—C14—H14A	109.6
C6—C5—C4	111.10 (12)	C15—C14—H14B	109.6
C6—C5—H5A	109.4	C13—C14—H14B	109.6
C4—C5—H5A	109.4	H14A—C14—H14B	108.1
C6—C5—H5B	109.4	C16—C15—C14	111.29 (12)
C4—C5—H5B	109.4	C16—C15—H15A	109.4
H5A—C5—H5B	108.0	C14—C15—H15A	109.4
C5—C6—C1	111.04 (12)	C16—C15—H15B	109.4
C5—C6—H6A	109.4	C14—C15—H15B	109.4
C1—C6—H6A	109.4	H15A—C15—H15B	108.0
C5—C6—H6B	109.4	C15—C16—C17	110.86 (12)
C1—C6—H6B	109.4	C15—C16—H16A	109.5
H6A—C6—H6B	108.0	C17—C16—H16A	109.5
C8—C7—C12	110.18 (11)	C15—C16—H16B	109.5
C8—C7—P1	111.69 (10)	C17—C16—H16B	109.5
C12—C7—P1	110.46 (10)	H16A—C16—H16B	108.1
C8—C7—H7	108.1	C16—C17—C18	111.30 (12)
C12—C7—H7	108.1	C16—C17—H17A	109.4
P1—C7—H7	108.1	C18—C17—H17A	109.4
C9—C8—C7	111.28 (12)	C16—C17—H17B	109.4
C9—C8—H8A	109.4	C18—C17—H17B	109.4
C7—C8—H8A	109.4	H17A—C17—H17B	108.0
C9—C8—H8B	109.4	C17—C18—C13	111.07 (12)
C7—C8—H8B	109.4	C17—C18—H18A	109.4
H8A—C8—H8B	108.0	C13—C18—H18A	109.4
C10—C9—C8	110.78 (13)	C17—C18—H18B	109.4
C10—C9—H9A	109.5	C13—C18—H18B	109.4
C8—C9—H9A	109.5	H18A—C18—H18B	108.0

C7—P1—C1—C6	173.93 (10)	P1—C7—C8—C9	−178.51 (10)
C13—P1—C1—C6	59.51 (11)	C7—C8—C9—C10	57.32 (17)
S1—P1—C1—C6	−64.79 (10)	C8—C9—C10—C11	−57.82 (18)
C7—P1—C1—C2	44.45 (12)	C9—C10—C11—C12	57.32 (17)
C13—P1—C1—C2	−69.97 (12)	C10—C11—C12—C7	−56.28 (16)
S1—P1—C1—C2	165.73 (9)	C8—C7—C12—C11	54.86 (16)
C6—C1—C2—C3	56.61 (16)	P1—C7—C12—C11	178.74 (10)
P1—C1—C2—C3	−173.43 (10)	C7—P1—C13—C18	−67.43 (12)
C1—C2—C3—C4	−56.03 (16)	C1—P1—C13—C18	47.06 (12)
C2—C3—C4—C5	55.46 (17)	S1—P1—C13—C18	170.45 (9)
C3—C4—C5—C6	−54.99 (17)	C7—P1—C13—C14	163.46 (10)
C4—C5—C6—C1	55.98 (16)	C1—P1—C13—C14	−82.05 (11)
C2—C1—C6—C5	−57.02 (16)	S1—P1—C13—C14	41.34 (11)

P1—C1—C6—C5	170.15 (10)	C18—C13—C14—C15	56.93 (16)
C1—P1—C7—C8	−179.57 (10)	P1—C13—C14—C15	−171.34 (10)
C13—P1—C7—C8	−61.26 (11)	C13—C14—C15—C16	−57.70 (16)
S1—P1—C7—C8	60.53 (11)	C14—C15—C16—C17	56.93 (17)
C1—P1—C7—C12	57.43 (11)	C15—C16—C17—C18	−55.49 (18)
C13—P1—C7—C12	175.73 (9)	C16—C17—C18—C13	55.34 (17)
S1—P1—C7—C12	−62.47 (10)	C14—C13—C18—C17	−55.97 (16)
C12—C7—C8—C9	−55.35 (16)	P1—C13—C18—C17	173.48 (10)

Hydrogen-bond geometry (Å, º)

D—H···*A*	*D*—H	H···*A*	*D*···*A*	*D*—H···*A*
C7—H7···S1^{i}	1.00	2.65	3.5961 (14)	157

Symmetry code: (i) *x*+1, *y*, *z*.